Supporting Information

Solar-driven photocatalytic reduction of copper(II) to copper(I) or zerovalent copper (Cu(0)): A sustainable approach for recovery of copper on a pilot scale

Sapana Jadoun[a,b*], Eduardo Aedo[a], Juan Pablo Fuentes[a,c], Jorge Yáñez[a*], Lorena Cornejo Ponce[d]
[a]Facultad de Ciencias Químicas, Departamento de Química Analítica e Inorgánica, Universidad de Concepción, 4070371 Edmundo Larenas 129, Concepción, Chile.
[b]Departamento de Química, Facultad de Ciencias, Universidad de Tarapacá, Avda. General Velásquez, 1775, Arica, Chile
[c]Departamento de Ciencias Básicas, Facultad de Ciencias, Universidad Santo Tomás, Buena Vecindad #91, Puerto Montt, Chile
[d]Departamento de Ingeniería Mecánica, Facultad de Ingeniería, Universidad de Tarapacá, Avda. General Velásquez 1775, Arica 1000007, Chile
*Corresponding author

Contents

Experimental Section

S 1. Materials

All reagents were procured from Merck, Germany. Photocatalysts for reducing copper included commercially available ZnO and previously synthesized POPD/ZnO nanohybrids, which were efficient adsorbents for Cu(II) ions.[1] As sacrifice reagents, formic acid (HCOOH) and oxalic acid ($H_2C_2O_4$) were used. Potassium chloride (KCl) facilitated the selective reduction to zerovalent copper, mitigating Cu(I) production. A stock solution of Cu(II) was prepared by dissolving analytical-grade copper sulphate ($CuSO_4{\cdot}5H_2O$) in ultra-pure water. Ethylenediaminetetraacetic acid (EDTA) and nitric acid (HNO_3) facilitated the quantitative extraction of adsorbed Cu(II). The presence of Cu(I) was detected using potassium thiocyanate (KSCN), resulting in the formation of a white precipitate of copper(I) thiocyanate (CuSCN) and dissolution in hydrochloric acid (HCl). Cu(II) concentrations were determined via FAAS at 324.8 nm. Ultrapure water, essential for all experiments, was obtained using an EASY water purification device (Millipore, US).

S2 Analytical determinations and analysis of Cu(0)

Dissolved Cu(II) concentrations were measured via FAAS at a wavelength of 324.8 nm. A standard calibration curve spanning 0-30 mg L^{-1} was constructed using standard Cu(II) reagents to facilitate this.[2] XRD analysis was conducted utilizing a Philips PW 3710 powder diffractometer (with nickel-filtered copper Kα radiation) within the 2θ range of 5˚-70˚ to identify the presence of Cu(I) and Cu(0). Spectral data were analyzed using the X'pert High Score Software and a database sourced from the Crystallography Open Database (COD).[3] Fluorescence spectra were obtained to capture the characteristic spectra of zerovalent copper, excited at 367 nm, with fluorescence detection at 420 nm.[4] EDX was employed to assess the purity of metallic copper.[5] LIBS analysis was conducted utilizing a Q-switched Nd-YAG laser (1064 nm, 50 mJ) procured from Litron, UK,

and a 6-channel spectrometer Aurora from Applied Spectra, CA, USA, per previous studies.[6] Data analysis was performed using LIBS spectral data acquisition software (Applied Spectra Inc., CA, USA). The surface morphology of ZnO before and after reduction was examined using FE-SEM (Leo Supra 50 V P, Carl Zeiss, Germany)

S 3. Quantitative measurement of reduction yield

Quantitative assessments of reduction yield were conducted to quantify the percentage recovery of zerovalent copper. Following the reduction process, all ionic copper species were extracted via complexation with 30 mL of EDTA (0.01 mol L^{-1}) under continuous stirring and subsequent sonication. This step facilitated the extraction and dissolution of all adsorbed and residual Cu(II) ions that remained unreacted during photoreduction.[7] The Cu(0) precipitate was dissolved via wet oxidation with 10 mL of HNO_3 (8 mol L^{-1}) at 85°C. This process transformed the red precipitate (Cu(0)) into a light blue transparent dissolution of Cu(II).[8] The resulting solution was diluted to 50 mL and subjected to analysis using FAAS.

S4. Quantitative analysis of Cu(I)

An HCl treatment was used to detect whether the final product was Cu(0), Cu(I), or simply adsorption on the surface of ZnO. Notably, Cu(0) remains insoluble in HCl, a non-oxidizing acid. On the contrary, Cu(I) dissolves as Cu_2O, transforming the system into a light blue transparent solution.[9] Moreover, the qualitative detection of Cu(I) was accomplished using KSCN, which forms a milky white precipitate of CuSCN upon binding with Cu(I) [10]. XRD analysis further confirmed this observation (discussed in the manuscript).

S5. Quantitative analysis of Cu(0)

The quantitative assessment of Cu(0) recovery was conducted through a series of sequential chemical treatments on the reduction product. Initially, EDTA was employed to chelate all Cu(II) present in the solution post-photoreduction.[11] Subsequently, acid digestion using HNO_3 was

utilized to convert all Cu(0) into Cu(II) to assess the concentration of photoreduced copper. Analysis of the remaining Cu(II) in the absence of EDTA revealed a concentration of only 3.27 mg L^{-1} via FAAS. However, EDTA extraction yielded 22.59 mg L^{-1} of Cu(II). Notably, when the process was conducted in the presence of a sonicator, the yield of Cu(II) (both in the filtrate and adsorbed Cu(II) on the surface of ZnO) increased to 41.36 mg L^{-1}. This enhancement can be attributed to the mechanical action of ultrasonic waves, facilitating the release of all adsorbed Cu(II) from the photocatalyst surface. This approach minimized errors and mitigated misinterpretations in the quantitative recovery of zerovalent copper (Table S3).

Alternatively, all the Cu(0) was separated via filtration and subsequently dried. Acid digestion using HNO_3 (8 mol L^{-1}) was then performed, converting all zerovalent copper to its ionic form for analysis using FAAS. The acid digestion studies revealed a concentration of 199.3 mg L^{-1} of Cu(II) from an initial Cu(II) concentration of 250 mg L^{-1}. This suggests a 79.72% recovery of zerovalent copper and a total Cu(II) recovery of 96.26% from its initial concentration after EDTA extraction and acid digestion process (Supporting Information, Table S4). In simpler terms, out of 50.00 mg, 39.86 mg was converted to zerovalent copper, while the remaining amount persisted as Cu(II) at the end of the process.

S6. Chloride promotes the selective photocatalytic reduction of Cu(II) to Cu(0)

Strategically tuning reaction conditions provides a practical way of directing reaction pathways and influencing product outcomes. In this context, chloride ions play a pivotal role in modulating the photoreduction process by forming chloride-copper complexes and acting as an additional sacrificial reagent. Potassium chloride (KCl) potential was investigated to introduce an additional element that could supply more electrons to facilitate photoreduction. Some literature suggests that chloride ions promote charge separation and enhance ionic strength, thereby increasing the availability of electrons. In contrast, others highlight using KCl to scavenge hydroxyl radicals

(OH°) from the system. These radicals could otherwise oxidize Cu(I) back to Cu(II), potentially hindering further reduction to Cu(0).[12]

The impact of KCl (0.1 g L^{-1}) was studied using three ways: (i) KCl alone, (ii) ZnO with KCl, and (iii) ZnO, formic acid, and KCl. Subsequent analysis of the resulting powdered products was conducted by dissolution in HCl. Interestingly, no significant enhancement in the reduction process was observed when KCl was used alone or with ZnO without formic acid. However, a notable improvement was noted when incorporated with ZnO and formic acid (Table S2, Supporting Information). However, the stage for adding KCl was also an important parameter studied. No improvement was seen when KCl was added with ZnO and formic acid at the start of the process. Still, when added after 20 minutes of formic acid, zerovalent copper was obtained at 90 minutes, which was insoluble in water and red in color. The concentration of Cu(II) was not increased after adding HCl, proving the presence of Cu(0) in the presence of ZnO, formic acid, and KCl, which was further confirmed by using XRD, FS, LIBS, and EDX analysis.

S7. Scalability of the concentration of Cu(II) ions during the photoreduction process

The scalability of processes concerning the concentration of Cu(II) was further investigated using GVRs under solar light conditions, with a fixed volume of 500 mL. Cu(II) concentrations ranging from 250 to 1000 mg L^{-1} were explored alongside varying concentrations of ZnO (2, 4, and 8 g L^{-1}), as illustrated in Fig S3.

During the initial 15 min of irradiation, a noticeable decrease in Cu(II) concentration was observed across all experimental setups. Subsequently, at intervals of 30, 45, 60, 75, and 90 min, metallic copper particles became evident in all cases. Notably, for concentrations up to 500 mg L^{-1}, the conversion of Cu(II) to Cu(0) surpassed that of the 1000 mg L^{-1} concentration within the same timeframe. However, over time, the Cu(II) concentration at 1000 mg L^{-1} also underwent a complete reduction to zerovalent copper, eventually falling below detection limits. This compelling finding

not only accentuates the efficiency of concentration-based scaling up of the process but also underscores the system's adaptability to handle varying Cu(II) concentrations under solar light irradiation.

These findings testify to the photoreduction process's efficiency and illustrate its potential for scalability across a range of Cu(II) concentrations. Moreover, using solar light to drive these transformations highlights the process's sustainability and underscores its alignment with environmentally friendly practices. By harnessing the sun's boundless energy, this approach paves the way for large-scale copper recovery endeavors that are economically viable and environmentally responsible.

S8. Recovery of copper via ultrasonication from the surface of the photocatalyst

Ultrasonication was employed to disperse the photocatalyst in the solvent and recover copper from their surface. This process involved subjecting the mixture containing the nanohybrids to high-frequency sound waves, inducing cavitation bubbles in the solvent. These bubbles rapidly expanded and collapsed, effectively releasing copper from the surface of the photocatalyst dispersed in the solvent. The metallic copper settled to the bottom of the reactor, enabling its recovery.

S9. Analysis of scalability and economic feasibility of SOLAR-Cu technology

Scaling the present technology from a laboratory or pilot setup to an industrial scale requires careful attention to reactor design, requirements of photocatalysts, solar light availability, and water source variability. Although RPRs show promise for handling large volumes, industrial applications may require reactors with capacities in the thousands of liters, posing challenges for maintaining uniform mixing and light distribution. The cost of the process includes reactors, photocatalysts, and solar light. Stable and continuous solar light is essential, and inconsistent sunlight may necessitate artificial lighting or hybrid systems, increasing costs. However, we used

natural solar lights in our experiments to scale up the study, which does not require additional cost. The availability and intensity of sunlight vary depending on geographical location, weather conditions, and time of year. Additionally, scaling up must address variations in water chemistry, as demonstrated by tests in distilled water, tap water, and seawater, which can influence process efficiency and control.

Cost analysis, compared to traditional methods, showed distinct advantages and challenges. Electrowinning, while cost-effective in areas with cheap electricity, demands high energy input and uses hazardous chemicals like sulfuric acid, contributing to environmental concerns. Hydrometallurgical recovery is efficient for low-grade ores but experiences high reagent costs and generates significant waste. In contrast, our process benefits from lower operational costs by utilizing solar energy and avoiding harsh chemicals. However, some initial costs are faced when setting up reactors; proper sunlight focuses on a wide reactor area, photocatalysts, etc. However, it's a fundamental step for sustainability and maintaining the circular economy to set up a large-scale recovery of copper using solar light.

Characterization

S10. Diffuse reflectance spectroscopy (DRS)

DRS was used to determine the absorption radiation range of the electromagnetic spectrum for photocatalysts. ZnO absorbs between 190 and 400 nm in the UV region due to the π -π* transition while absorbing negligible visible light radiation, Fig S2.[13]

S 11. SEM analysis

SEM images for the ZnO without copper and with copper on its surface before extraction are shown in Fig S4. Before the reduction process, the SEM images depicted a pristine surface of ZnO characterized by its delicate, well-shaped features with specific dimensions. However, after the

reduction, the surface of ZnO appeared littered with whitish nodules of copper. This dramatic change in surface morphology suggests a profound alteration in the structural integrity of the ZnO material following the reduction of copper. It also indicated the presence of a lot of irregular surfaces with swollen and highly porous structures. These changes suggest that reducing copper on the ZnO surface has induced significant structural changes, potentially altering its physical properties and surface characteristics. The formation of these porous structures may be attributed to the deposition of copper nanoparticles, which could catalyze the growth of ZnO crystals in non-uniform patterns or induce surface roughening through chemical interactions.

References

(1) Jadoun, S.; Fuentes, J. P.; Urbano, B. F.; Yáñez, J. Highly Efficient Remediation of Cu (II) from Water by Novel Poly(o-Phenylenediamine)/Zinc Oxide Nanohybrids: Kinetic, Equilibrium, and Thermodynamic Studies. *J. Water Process Eng.* **2023**, *53*, 103663. https://doi.org/https://doi.org/10.1016/j.jwpe.2023.103663.

(2) Bagherian, G.; Arab Chamjangali, M.; Shariati Evari, H.; Ashrafi, M. Determination of Copper (II) by Flame Atomic Absorption Spectrometry after Its Perconcentration by a Highly Selective and Environmentally Friendly Dispersive Liquid–Liquid Microextraction Technique. *J. Anal. Sci. Technol.* **2019**, *10*, 1–11.

(3) Khokhar, D.; Jadoun, S.; Arif, R.; Jabin, S.; Budhiraja, V. Copolymerization of O-Phenylenediamine and 3-Amino-5-Methylthio-1H-1, 2, 4-Triazole for Tuned Optoelectronic Properties and Its Antioxidant Studies. *J. Mol. Struct.* **2021**, *1228*, 129738.

(4) Wang, N.; Ga, L.; Ai, J.; Wang, Y. Fluorescent Copper Nanomaterials for Sensing NO2− and Temperature. *Front. Chem.* **2022**, *9*, 1211. https://doi.org/10.3389/FCHEM.2021.805205/BIBTEX.

(5) Lange, B.; Recknagel, S.; Czerwensky, M.; Matschat, R.; Michaelis, M.; Peplinski, B.; Panne, U. Analysis of Pure Copper–a Comparison of Analytical Methods. *Microchim. acta* **2008**, *160*, 97–107.

(6) Velásquez, M.; Álvarez, J.; Sandoval, C.; Ramírez, E.; Bravo, M.; Fuentes, R.; Myakalwar, A. K.; Castillo, R.; Luarte, D.; Sbarbaro, D.; Yáñez, J. Improved Elemental Quantification in Copper Ores by Laser-Induced Breakdown Spectroscopy with Judicious Data Processing. *Spectrochim. Acta Part B At. Spectrosc.* **2022**, *188*, 106343. https://doi.org/https://doi.org/10.1016/j.sab.2021.106343.

(7) Kumar, R.; Barakat, M. A.; Daza, Y. A.; Woodcock, H. L.; Kuhn, J. N. EDTA Functionalized Silica for Removal of Cu (II), Zn (II) and Ni (II) from Aqueous Solution. *J. Colloid Interface Sci.* **2013**, *408*, 200–205.

(8) Mecucci, A.; Scott, K. Leaching and Electrochemical Recovery of Copper, Lead and Tin from Scrap Printed Circuit Boards. *J. Chem. Technol. Biotechnol. Int. Res. Process.*

Environ. Clean Technol. **2002**, *77* (4), 449–457.
(9) Tran, T. T.; Moon, H. S.; Lee, M. S. Separation of Cobalt, Nickel, and Copper from Synthetic Metallic Alloy by Selective Dissolution with Acid Solutions Containing Oxidizing Agent. *Miner. Process. Extr. Metall. Rev.* **2022**, *43* (3), 313–325.
(10) Wu, W.; Jin, Z.; Hua, Z.; Fu, Y.; Qiu, J. Growth Mechanisms of CuSCN Films Electrodeposited on ITO in EDTA-Chelated Copper (II) and KSCN Aqueous Solution. *Electrochim. Acta* **2005**, *50* (11), 2343–2349.
(11) Zhao, J.; Hu, X.; Kong, L.; Peng, X. UV Irradiation Induced Simultaneous Reduction of Cu (II) and Degradation of EDTA in Cu (II)-EDTA in Wastewater Containing Cu (II)-EDTA. *J. Hazard. Mater.* **2024**, *465*, 133131.
(12) Iguchi, S.; Teramura, K.; Hosokawa, S.; Tanaka, T. Effect of the Chloride Ion as a Hole Scavenger on the Photocatalytic Conversion of CO 2 in an Aqueous Solution over Ni–Al Layered Double Hydroxides. *Phys. Chem. Chem. Phys.* **2015**, *17* (27), 17995–18003.
(13) Ramírez, A. E.; Montero-Muñoz, M.; López, L. L.; Ramos-Ibarra, J. E.; Coaquira, J. A. H.; Heinrichs, B.; Páez, C. A. Significantly Enhancement of Sunlight Photocatalytic Performance of ZnO by Doping with Transition Metal Oxides. *Sci. Rep.* **2021**, *11* (1), 2804.

Table S 1.Optimization of pH for photoreduction of Cu(II) to Cu(0)

	Initial pH: 3		Initial pH: 4		Initial pH: 5		Initial pH: without adjustment	
Time (min)	Without light	With light	Without light	With light	Without light	With light	Without light	With light
0	3.04	3.01	4.01	4.02	5.02	5.04	5.25	5.26
1	3.75	4.69	5.96	6.01	5.98	6	6.01	6.05
5	4.21	4.55	6.21	6.31	6.32	6.27	7.15	7.19
10	4.86	5.02	6.42	6.53	6.55	6.45	7.38	7.32
15	5.26	5.98	6.25	6.37	6.31	6.25	7.05	7.12
30	5.88	6.27	6.27	6.35	6.37	6.27	6.29	6.27
45	6.33	6.28	6.31	6.29	6.24	6.28	6.25	6.27
60	6.76	6.45	6.24	6.28	6.25	6.26	6.26	6.27

Table S 2.Acid digestion using HCl for confirmation of the presence of Cu(0)

	KCl added at the start of the process		KCl added after 15 min of formic acid addition	
	Absence of KCl	Presence of KCl	Absence of KCl	Presence of KCl
Concentration of Cu(II) after dissolving final powder in HCl (mg L^{-1})	245.3	241.2	246.4	23.86

Table S 3.Quantitative analysis of leftover concentration of Cu(II) after photoreduction

Process	Concentration of Cu(II) after reduction (mg L^{-1})
In the absence of EDTA	3.267
In the presence of EDTA	22.59
In presence of EDTA and sonicator	41.36

Table S 4.Total recovery of copper by EDTA extraction and acid digestion

Initial Cu(II) (mg L^{-1})	**Cu(II) Concentration (mg L^{-1}) after photoreduction**		**% Recovery of Cu(0)**	**% Recovery of initial Cu(II)**
	EDTA extraction Cu(II)	Acid digestion by $HNO_{3\,(conc)}$ Cu(0)		
250	41.36	199.3	79.72	96.264

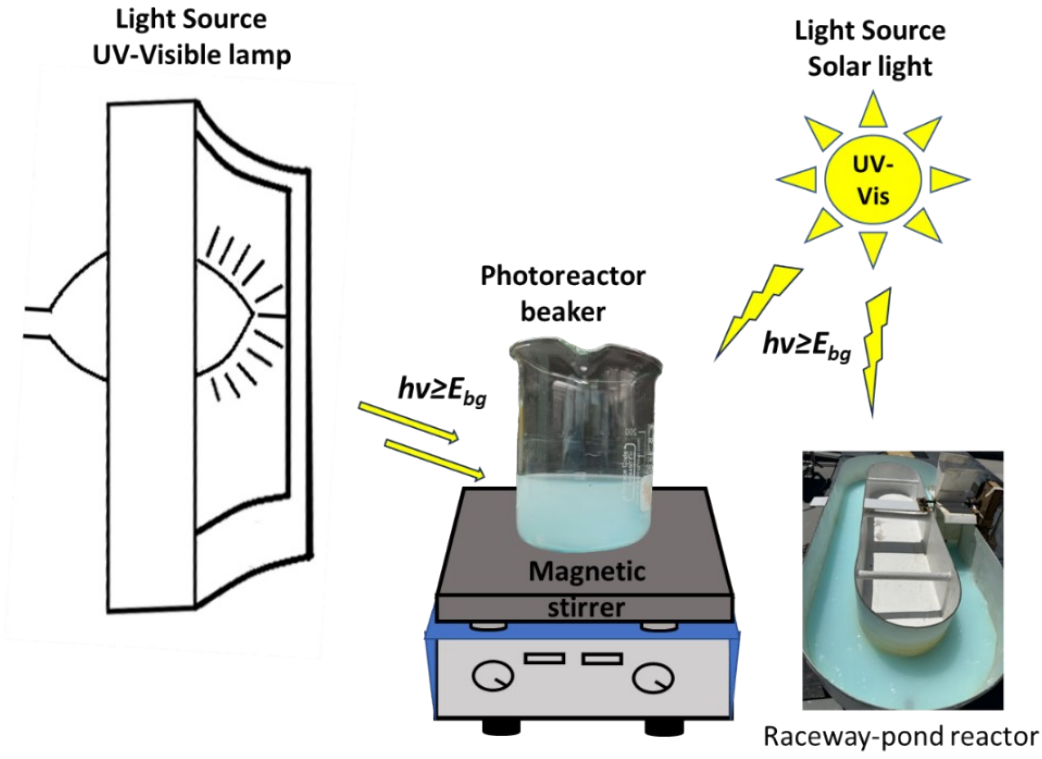

Fig S 1.Experimental setup for the solar photocatalytic reduction of copper under the solar lamp/solar light with complete photoreduction process using glass vessel reactors and raceway pond reactor

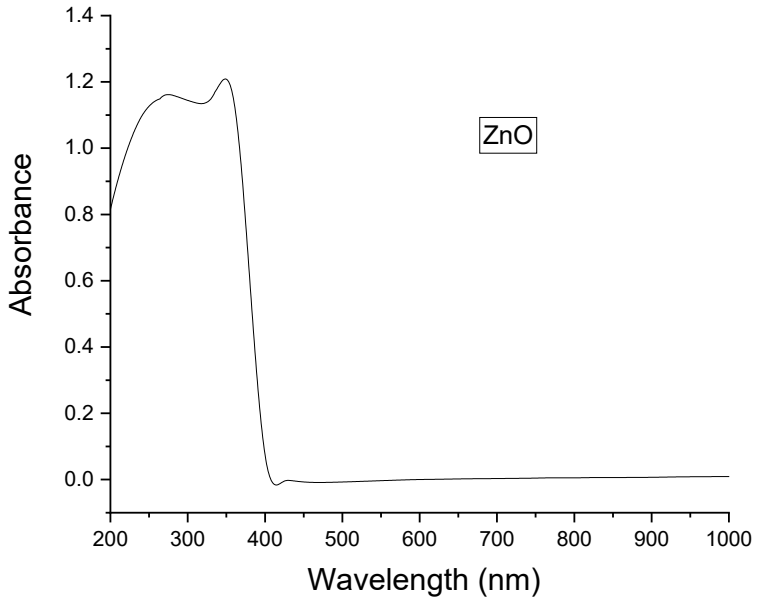

Fig S 2. Diffuse Reflectance Spectra of zinc oxide (ZnO)

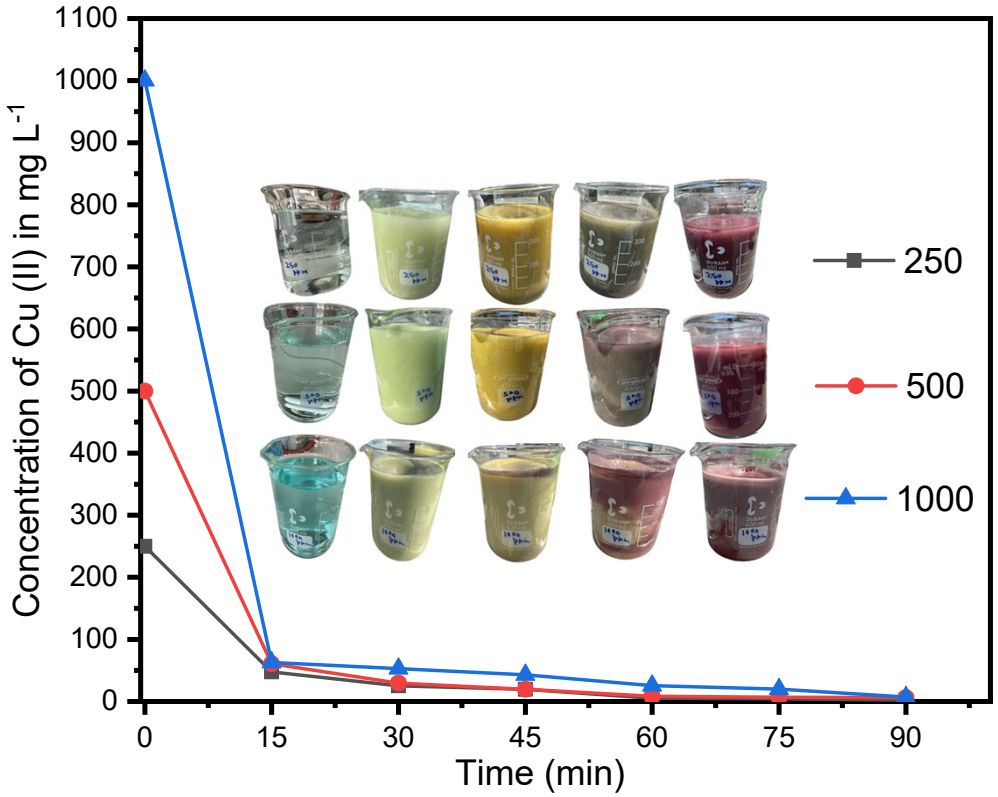

Fig S 3.Scaling up of process in terms of concentration of copper ions (250, 500, and 1000 mg L^{-1}) in solar light.

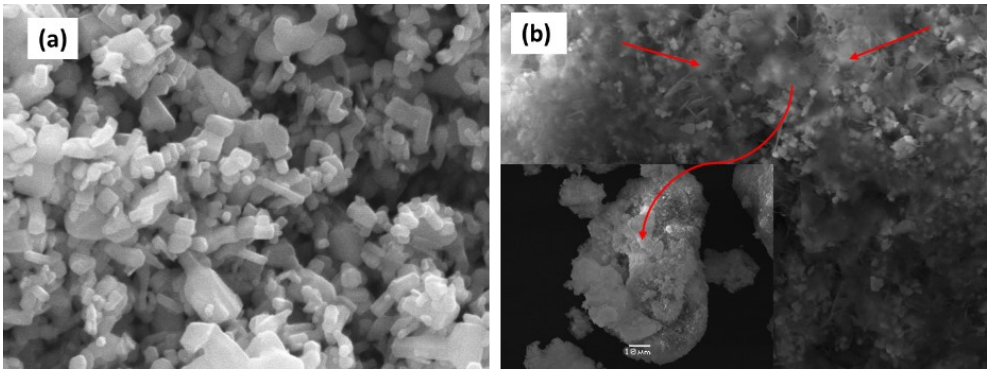

Fig S 4.SEM images of (a) pristine ZnO and (b) reduced zerovalent copper on the surface of the ZnO

Video S1. Photoreduction of copper in GVR.mp4

Video S1. Photoreduction of copper in Glass Vessel Reactors

Video S2. Photoreduction of copper in RPR.mp4

Video S2. Photoreduction of copper in Raceway Pond Reactors

Video S3. Hyperlapse Video_RPR_Reduction of Cu.mp4

Video S3. Hyperlapse video of photoreduction of copper in Raceway Pond Reactors